Title: Soil modeling for soil loss tolerance estimations: exploring natural baselines and long-term variations

Authors: Keerthika N. Ranathunga [a, b,*], Peter A. Finke [a], Qiuzhen Yin [b], Ann Verdoodt [c], YanYan Yu [d]

Affiliations:

[a] Department of Environment, Research group of soilscape genesis, Ghent University, Coupure links 653, B-9000 Ghent, Belgium (KeerthikaNirmani.Ranathunga@UGent.be, Peter.Finke@UGent.be)

[b] Earth and Life Institute, Georges Lemaitre Center for Earth and Climate Research, Université Catholique de Louvain, Place Louis Pasteur 3, B-1348 Louvain-la-Neuve, Belgium (qiuzhen.yin@uclouvain.be)

[c] Department of Environment, Research group of soil degradation and conservation, Ghent University, Coupure links 653 Ghent, B-9000 Belgium (Ann.Verdoodt@UGent.be)

[d] Institute of Geology and Geophysics, Chinese Academy of Sciences (IGGCAS), 19, Beitucheng Xilu, Chaoyang District, 100029, Beijing, China (yyy@mail.iggcas.ac.cn)

*Corresponding author: Keerthika N. Ranathunga

Research group of soilscape genesis, Ghent University, Coupure links 653, B-9000, Ghent, Belgium KeerthikaNirmani.Ranathunga@UGent.be, Peter.Finke@UGent.be

Phone +32 926 4 6052

Citation- Ranathunga, K. N., Finke, P. A., Yin, Q., Verdoodt, A., & Yu, Y. (2021). Soil modeling for soil loss tolerance estimations: Exploring natural baselines and long-term variations. In: Global and Planetary Change, Vol 204, p. 103548 (2021)

https://doi.org/10.1016/j.gloplacha.2021.103548

Abstract

Quantification of soil stocks and ecosystem services (ES) under changing climate need time series of climate and soil data. Here, we propose a new approach combining process-based soil and climate simulations to obtain such time series, and apply it onto a recent interglacial, Marine Isotope Stage (MIS) 5e.

We combined the LOVECLIM climate model and the SoilGen2 soil evolution model to simulate soil development under two scenarios: dust addition plus erosion and erosion-only (both with five erosion rates corresponding to low, natural erosion rates: 0, 0.5, 1.0, 1.5 and 2.0 Mg ha^{-1} y^{-1}). We quantified five target variables: two soil stocks, Exchangeable Bases (EB) and Soil Organic Carbon (SOC), and three ES: Carbon Sequestration Capacity (CSC), Water Yield (WY) and the ratio of actual over potential evapotranspiration (Ω) at four sites on an aridity gradient on the Chinese Loess Plateau (CLP). We used the obtained time series of these target variables to estimate Soil Loss Tolerance (SLT) threshold values over the full extent of MIS 5e (22 ka).

Under increased erosion, EB increases while SOC always declines in both scenarios.
In both scenarios, the simulated CSC increases with erosion; contrastingly, the WY decreases with increasing erosion rates. Both CSC, WY and Ω gradually decrease towards the northwest CLP (semi-arid region). For EB and SOC, the determined SLT thresholds are relatively higher in the dust addition than in the erosion-only scenarios, and strictly follow the climate gradient in the CLP. Combined performance index for (1-CSC), WY and Ω, showed that soil ES performance is worse above 1.0 Mg ha^{-1} y^{-1}. This implies that benchmark levels must be chosen carefully.
Our research highlights the potential of using SoilGen2 with LOVECLIM for quantifying soil-based ES and SLT.

Key words: Chinese loess plateau; exchangeable bases; soil organic carbon; carbon sequestration capacity; water yield; Last Interglacial

1. Introduction

Soil is an important non-renewable natural resource and is recognized essential to sustainable development as it renders vast benefits to living beings (Bouma, 2014). These benefits, known as ecosystem services (ES), are classified into four groups: (i) provisioning services (e.g. food, fiber, fuel and fresh water for living beings), (ii) regulating services (e.g. regulating carbon sequestration, erosion control, water purification), (iii) cultural services (e.g. spiritual, religious, educational, recreation and tourism) and (iv) supporting services (e.g. nutrient cycling, habitat reservoir) (Costanza et al., 1997; DeGroot et al., 2002; MEA, 2005).

Dominati et al. (2010) defined the complex relationship between soil and ES by adopting the concept of natural capital. The soil natural capital represents soil stocks (= soil properties expressed on a mass basis) and constitutes the basis for providing soil-based ecosystem goods and services. Soil natural capital is characterized by both inherent (naturally inborn) and manageable properties. Inherent soil properties (e.g. soil depth, slope, texture) are stable properties that are unlikely to change at short-term (but likely at long-term) while manageable soil properties (e.g. soil organic matter, exchangeable bases) are changeable and can be modified through management practices. At long term, we define soil depth as a dynamic soil property, as a variable measure, that is influenced by soil formation factors and environmental conditions. For example, soil erosion decreases soil depth by topsoil removal and, consequently, topsoil organic matter stocks decline.

Soil formation (positive contribution) and degradation (negative contribution) processes underpin the soil natural capital, which subsequently affects the beneficial flows of soil stocks, i.e. the soil-based ES. Many authors have highlighted and agreed that the four groups of ES largely rely on soil (e.g. Bouma, 2014; Daily et al., 1997; Dominati et al., 2014, 2010) and many different soil-based methodologies and frameworks have been initiated (e.g. Calzolari et al., 2016; Fossey et al., 2020; Hewitt et al., 2015; Rutgers et al., 2012). Adhikari and Hartemink (2016) reviewed extensive literature on the transfer of key soil properties to ES.

Additionally, authors (e.g. Dominati et al., 2010; Greiner et al., 2017) suggest that soil properties are not comprehensively studied in soil-related ES assessments. On the other hand, handling temporal variations of ES must involve dynamically changing soil properties instead of using fixed values (ex: concentration, measurement) collected at one time point. Furthermore, most of the ecosystem studies depend on soil databases, measurements and covering only few years or decades and long-term evolution of ecosystem services and soil stocks is hardly known due to paucity of legacy data. To better quantify soil-based ES in long-term ES assessments, mathematical modeling of soil development comes as a potential promising alternative (to inventories of soil stocks). It furthermore offers a robust approach to study future ES changes and trends under climate change and human population induced land use and land management change. Process-based, dynamic soil models were highlighted as essential tools in assessing ES (Greiner et al., 2017). Several examples of soil modeling studies have been reported for quantifying ES (see table 2 in Vereecken et al., 2016) and by Lu et al. (2015).

The Chinese Loess Plateau (CLP) is one of the most erodible areas in the world. Our selections were based on ES studies, which describe ecological constraints in the CLP. In the topsoil, loss of soil nutrients and Soil Organic Carbon (SOC) have been widely discussed in response to water erosion (Cai, 2001; Li et al., 2016; Liu et al., 2011). These soil nutrients (=exchangeable bases), which are commonly regarded and evaluated for understanding the nutrient provision potential for plants in the ES frameworks (DeGroot et al., 2002; MEA, 2005), are included as a soil stock. Carbon Sequestration Capacity (CSC) (together with SOC stocks) and Water Yield (WY) have been intensively assessed in various aspects through different methodologies by various researches in numerous case studies at local, regional and watershed scales, as they are conceived as very important ES in this region vulnerable to water erosion (Feng et al., 2020; Lang et al., 2017; Lu et al., 2015; Su et al., 2018, 2012; Yin et al., 2020).

Modeled climate time series data are essentially required as input in soil models. As climate plays a dominant role in soil natural capital formation, a clear understanding of how soil-based ES relate to climate dynamics is needed, and this research gap remains to be filled. Climate change likely influences ES, either positively (by developing soil stocks) or negatively (by degrading soil stocks). To our knowledge, no comprehensive long-term (millennium time scale) study has been conducted in a natural ecosystem with an advanced soil genesis model in combination with a climate model.

Nonetheless, the major external-inputs (e.g. soil erosion and deposition) are equally important to consider. Aeolian dust deposition in the CLP can increase the nutrient content and thickness of the existing surface soils. Deposition of thin layers of dust may contribute positively to the soil stocks by mixing with the existing soils (Kemp, 2001). Soil erosion is input as external-input during the study.

Regarding soil erosion, to distinguish human-caused accelerated erosion (i.e. rates exceeding soil formation rate) from natural erosion rates in terms of consequences for soil performance, terms like "permissible rates of soil erosion", "natural erosion levels", and "Soil Loss Tolerance (SLT)" have been employed (Boardman and Poesen, 2006; Li et al., 2009; Nearing et al., 2017).

Specifically, Verheijen et al. (2009) proposed to define SLT with reference to soil functions. According to the authors, SLT is "any actual soil erosion rate at which a deterioration or loss of one or more soil functions does not occur"— actual soil erosion being "the total amount of soil lost by all recognized erosion types". Furthermore, the concept of SLT has been extensively applied not only for these on-site impacts but also to prevent off-site consequences by water erosion (e.g. sediment deposition and composition, flood control, water quality) and is being implemented in sustainable soil conservation strategies (Bazzoffi, 2009; DiStefano and Ferro, 2016; Li et al., 2009). In this study, in a natural context and using a pedon-scale model, erosion is considered as an external-input and therefore common erosion models are not used, which are particularly employed for erosion assessment on arable lands.

Usually, both SLT and ES are studied from an anthropocentric perspective (Bouma, 2014) to evaluate how they fulfill human needs in a sustainable way. However, there are good reasons for evaluating ES and SLT in natural ecosystems with zero human influence: (i) to be set as a benchmark for anthropocentric study in the future use, while (ii) checking if a sensitivity of ES-performance to varying natural erosion rates exists, taking into account climate variability. The above considerations motivated us to study long-term evolution of the soil natural capital in a natural ecosystem by modeling both climate dynamics and soil development under various low (natural) rates of erosion to answer the following questions:

(i) What are natural fluctuations in the soil stocks and ES?
(ii) How are these related to natural (low) soil erosion rates?

If soil functioning would be found to have a marked change at certain low erosion rates, then a next question would be:

(iii) What are SLT values for particular soil functions in natural ecosystems?

To answer the above questions, we combine a mechanistic soil development model, SoilGen2 (Finke, 2012; Finke and Hutson, 2008) with a climate model of intermediate complexity, LOVECLIM (Goosse et al., 2010) to estimate how soil stocks and ES fluctuated in one of the warmest Quaternary interglacials, MIS 5e.

This leads to the following objectives:

1. To quantify two soil stocks: soil organic carbon (Mg/ha) and exchangeable bases (kmol+/ha) and three ES: water yield (mm), the ratio actual/potential evapotranspiration (Ω) and carbon sequestration capacity (Mg/ha).
2. To assess the effect of various natural (low) erosion rates on soil stocks and ES and thus identify SLT via modeling.
3. To assess the effect of a geographic climate gradient on soil stocks, ES and SLT.

In this study, we focus on the CLP, because soils dating back to past interglacials are well-preserved there, and at present, major erosion problems occur (Feng et al., 2016; Shi and Shao, 2000) that motivate research including the definition of baseline levels of erosion and SLT-estimates. The underlying assumption is that studies based on modeling are an alternative to the more common inventory-based studies on soil natural capital and ES and can additionally be used for prediction and for identification of SLT threshold levels.

2. Material and Methods

2.1 Study area

The study area is the loess plateau (30°–40°N, 105°–115°E) in the north-central part of China. The loess there contains complete loess-soil alternations dating back to the early Miocene (Guo et al., 2002). During the Quaternary, more than 30 paleosols have formed during interglacials in the loess and were buried below loess added during glacial periods (Ding et al., 2002; Kukla, 1987; Liu, 1985). These paleosols explicitly show the paleo-environmental changes, mostly resulting from long-term variations in the East Asian Monsoon (EAM) (An et al., 1990; Liu, 1985). On the CLP, loess is an Aeolian dust material originating from northern and northwestern deserts and piled up during glacial periods, associated with the East Asian Winter Monsoon (EAWM). During interglacials, the intensified East Asian Summer Monsoon (EASM) brought moisture and heat to the loess plateau under continued but lower dust addition levels. Pedogenesis occurs during these more humid and warmer conditions (Guo et al., 2000). In glacial periods, pedogenesis slows down and dust deposition increases, which leads to buried soils, the so-called paleosols. Soils at the surface of the loess plateau are denoted by S0, the Holocene soil layer, which is underlain by a massive and yellowish loess unit L1 (Malan loess) deposited during last glacial period. Below L1, the S1 paleosol unit was formed during the last interglacial (An et al., 1991; Liu, 1985). These loess and paleosol layers have been well documented by numerous studies on various soil properties, such as mineralogical (e.g. Jeong et al., 2011), magnetic properties (e.g. An et al., 1991; Hao and Guo, 2005; Maher and Thompson, 1991), geochemical properties (e.g. Han et al., 1998; Jun et al., 1998; Xiong et al., 2010), grain size (e.g. Ding et al., 2002; Yang and Ding, 2008) and isotopic properties (e.g. Yang et al., 2012).

The present climate of the loess plateau is also monsoon-dominated with a clear climate gradient ranging from the warm-humid climate of the southeast to the cold-dry climate in the northwest. Mean annual temperature varies from 8°C in the northwest to 14°C in the southeast. Mean annual precipitation is around 300 mm in the northwest and increases to nearly 700 mm towards the southeast (Jiang et al., 2014), and is concentrated in the summer months July, August and September. The large precipitation gradient gives rise to a change in vegetation. There are five vegetation zones; from the northwest to the southeast, these are desert, desert-steppe, steppe, forest-steppe and forest (Yamanaka et al., 2014).

We focus on four paleosol sections– from northwest to southeast – Jingyuan, Xifeng, Luochuan and Chang'an (Fig. 1).

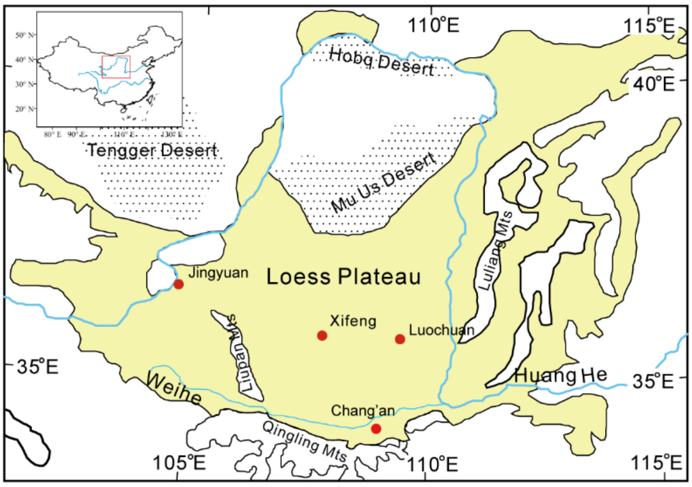

Figure. 1. Single column fitting image

Fig. 1. Geographic locations, from southeast to northwest Chang'an (34.17° N, 108.95° E), Luochuan (35.70° N, 109.40° E), Xifeng (35.70° N, 107.60° E), and Jingyuan (36.38° N, 104.62° E) in the CLP. Modified after Hao and Guo (2005).

2.2 Study period

We evaluate the effect of soil erosion in a "natural environment". Therefore, the last interglacial, MIS 5e (133-111 ka BP), was selected because it is one of the warmest interglacials during the Quaternary and is considered to some degree as an analogue to the future climate (Yin and Berger, 2012). Furthermore, for MIS 5e no assumptions about the (history of) land use have to be made since only natural vegetations occurred.

2.3 Climate model

LOVECLIM (Goosse et al., 2010), a three-dimensional Earth system model of intermediate complexity, was used to simulate the paleoclimate of the sites. Time series of monthly mean temperature (T), precipitation (P) and potential evapotranspiration (Ep) were input in the SoilGen2 (see details in supplementary material). LOVECLIM has been used in many studies for past and future climate. It has been used to simulate the EASM during MIS 13 (Yin et al.,

2009) and its results were confirmed by more complex climate models like HadCM3 (Muri et al., 2013). It has also been used to simulate the climate of the last nine interglacials of over the last 800 ka (Yin and Berger, 2015, 2012).

2.4 Soil model

In order to calculate the soil stocks and ES, the long-term (22 ka) evolution of soil chemical, physical and biological properties and processes were simulated with the SoilGen2 model (Finke, 2012; Finke and Hutson, 2008). SoilGen2 simulates multiple soil processes and their interrelations concomitantly and is thus a suitable tool for our study. It depicts major processes and time steps for individual soil processes inside the model ranging from seconds to a year. Evolution of more than 80 soil properties is output for every simulated year per compartment. Essentially, the pedogenetic model calculates the development of a large number of soil properties and stocks by quantitative process descriptions driven by both initial and time-variant boundary conditions. These boundary conditions reflect the soil formation factors ("CLORPT"; Jenny, 1941). The initial and boundary soil conditions that were used in this study are presented in the supplementary information. An in-depth description of the SoilGen2 model and its model concept, components and processes is in the user manual for SoilGen 2.26 (Finke, 2020).

The model was verified against measurements in various other sites for different soil processes (Finke et al., 2021, 2015; Keyvanshokouhi et al., 2016; Sauer et al., 2012; Yu et al., 2013; Zwertvaegher et al., 2013) and performance was satisfactory. Recently, Finke et al. (2018) compared uncertainty due to model inaccuracies to uncertainty due to soil spatial variability, and it was concluded that both sources were equally important and of low magnitude. Highly relevant to the current study, Finke et al. (2017) modeled soil development in MIS 5e and MIS 13 at eight sites along a climate gradient with documented paleosols in the Chinese loess under a LOVECLIM- simulated interglacial climate.

2.5 Soil stocks, ES and scenario

Two major scenarios were applied: one with dust addition combined with soil erosion and the other with only soil erosion (no dust addition). Dust addition rates are based on reconstructions for MIS 5e by (Lu and Sun, 2000) and are between 10-50 mm/ka in Southeast and Northwest CLP respectively. Twenty runs were simulated for each scenario: five soil erosion rates for four sites for assessing Soil Loss Tolerance (SLT). Supplementary material of this article provides a comprehensive methodology for how dust addition and water erosion are (table S2) used as model external-inputs.

2.5.1 Soil organic carbon

SoilGen2 simulates the mass of organic carbon (Mg/ha) per five-cm compartment, for each year over the total period. This output is aggregated over the top 30 cm. The topsoil organic carbon stock (SOC) then follows from [1]

$$\mathrm{SOC}(Mg/ha) = \sum_{c=1}^{6}(SOC_c) \qquad [1]$$

Where SOC_c indicates simulated mass of Soil Organic Carbon (Mg/ha) per depth of five cm.

2.5.2 Exchangeable bases

The exchangeable bases (EB) is defined as the sum of the macronutrients calcium (Ca), magnesium (Mg), potassium (K) and sodium (Na) on the exchange complex. It thus represents that part of the Cation Exchange Capacity (CEC) occupied by exchangeable bases. The CEC is in SoilGen2 a variable of the clay and organic matter content. SoilGen2 aggregates the exchangeable bases for each year over 30 cm as in [2]:

$$\mathrm{EB}\ (\frac{kmol+}{ha}) = \sum_{c=1}^{6}(\mathrm{XCa}_c+\mathrm{XMg}_c+\mathrm{XK}_c+\mathrm{XNa}_c) \times \rho_c \times 0.5 \qquad [2]$$

Where EB represents the summation of major exchangeable basic cations, XCa_c, XMg_c, XK_c, and XNa_c in mmol+/kg soil in compartment c (5 cm), ρ_c is the bulk density (kg/dm^3) in this compartment and 0.5 is the conversion factor from mmol+/kg to kmol+/ha, accounting for compartment thickness. The soil bulk density varies in the soil compartment over time, however the model assumes constant volume in each soil compartment during simulations.

2.5.3 Carbon Sequestration Capacity

Concerning the carbon sequestration capacity (CSC), as stated by many authors (Angers et al., 2011; Feng et al., 2013; Six et al., 2002; Stewart et al., 2007), the capacity to sequester additional SOC in soils is the difference between the maximum “theoretical” capacity and current SOC level in the soil's fine particles. Following this view, we use the Hassink (1997) approach to define the maximum carbon-saturation in the simulated soils, and the difference between the amount SOC already present and the maximum in the upper 30 cm in soil was used for CSC estimation.

The maximum carbon storage in a soil is defined here by the carbon saturation level (C*sat*, g/kg soil). *Csat* is calculated in each simulation year by using the protocol that has been derived by Hassink (1997):

$$C_{sat}\left(\frac{g}{kg}\right) = 4.09 + 0.37 \times (\%\, particles < 20\mu\, m) \qquad [3]$$

Equation [3] describes the total carbon in soil associated with soil particles less than 20 µm, thus the clay and part of the silt fractions, which change due to soil development processes. Then, CSC (Mg/ha) is estimated as follows for the upper 30 cm of soil:

$$\mathrm{CSC}(Mg/ha) = \sum_{c=1}^{6}\left(\left(C_{sat_c} \times \rho_c \times 0.5\right) - SOC_c\right) \qquad [4]$$

Where, ρ is the bulk density (kg/dm^3), which is also a variable. 0.5 is used as unit conversion to Mg/ha per compartment (c) of 0.05 m. SOC_c (Mg/ha) is the soil organic carbon stock in a particular year. CSC (Mg/ha) is calculated through the difference between C_{sat} and SOC in that year.

2.5.4 Water yield

In the evaluation of ES, water can perform functions such as either water regulation (e.g. control floods) or water supply (e.g. plant available water content) (Dominati et al., 2010) and these are very strongly linked. Here we consider water yield (WY) the loss of water below the root zone, and the ratio actual/potential evapotranspiration (Ω) to indicate plant water stress. We estimate how much water leaves the soil profile (=drainage), after plant water uptake, surface evaporation and interception evaporation associated with vegetation type. We take as root zone the upper 1m of soil depth, corresponding to the deepest root zone of the possible vegetation types (i.e. that of deciduous forest). We calculated overland flow by considering all non-infiltrating water to be runoff and assumed that both overland flow and drainage below the root zone contribute to basins, rivers and ground water recharge. However, since SoilGen2 is a 1-D model we did not simulate the flowpaths of water lost from the soil profile, as in landscape-scale studies.

Model runs showed that the long-term average surface runoff was less than 1% of the net precipitation for both scenarios (dust+erosion and only erosion) for both the most arid and the least arid plots. The low surface runoff was due to the high (natural) vegetation cover and flat terrain position in the simulated plots as well as the high infiltration capacity of the loess soils relative to the rainfall intensity. Then, annual water yield (=drainage) can simply be calculated as follows:

$$\text{WY}\ (mm) = P - \sum_{t=0}^{365}\sum_{c=1}^{20} Ea_{tc} \qquad [5]$$

Where P stands for the annual precipitation (mm), (site level precipitation) and Ea_{tc} is the actual evapotranspiration (mm), which is summed over 20 compartments c 1m) and per day t.

Then, to estimate how much water is available for plants (Ω) we use the potential evapotranspiration (Ep) from LOVECLIM on an annual basis, thus we obtain:

$$\Omega(-) = {\sum_{t=0}^{365}\sum_{c=1}^{20} Ea_{tc}}\Big/{Ep} \qquad [6]$$

2.5.5 Assessing the soil loss tolerance

Various definitions of SLT have been adopted in the past (Alewell et al., 2015; Boardman and Poesen, 2006; Duan et al., 2017; Li et al., 2009; Sparovek and De Maria, 2003; Wischmeier and Smith, 1979). Given the natural setting in our study, the most appropriate legacy definition of SLT is the soil erosion rate that equals more or less the soil formation rate. Thus, SLTs are usually derived through soil formation rates from bedrock material. However, for specific environments such as loess deposits, parent material for interglacial soil, estimating SLT value is very tricky, because it has no relation to the underlying bedrock. Therefore, we refine this definition by setting the SLT at that rate of erosion above which a deterioration of soil stocks and ES performance occurs. An erosion rate of 2.0 Mg ha^{-1} y^{-1} is considered the upper limit of natural erosion rates in the CLP where plateau landscape is assumed and simulated and include 5 erosion rates: no erosion, 0.5, 1.0, 1.5 and 2.0 Mg ha^{-1} y^{-1}. The selected erosion rates are very small (insignificant) compared to accelerated soil erosion rates. Human-induced accelerated erosion did not occur during MIS 5e, which motivates our choice of erosion rates and our selections accord with natural and geologic erosion rates as reported by Granger et al. (1996), Wilkinson and McElroy (2007), Nearing et al. (2017, in there table 1). Moreover, we assume that these minimum natural erosion rates gradually continue over a very long period (22 ka) (although the model does this pulsewise by removing soil compartments).

We obtain SLT by evaluating how much the stock, over MIS 5e, responds to various erosion rates, and identifying at what erosion rate a marked change occurs (this was identified based on cumulative amount). A marked change is visually identified when the difference of a stock between two adjacent erosion rates is clearly larger than the difference between two other adjacent erosion rates, e.g. the difference between rates 1.5-2.0 is larger than that between 1.0 and 1.5 Mg ha^{-1} y^{-1}. Potentially, each individual soil stock and ecosystem service may lead to a different SLT. Therefore, we propose to combine performance indicator based on the three quantified ES as follows:

1. For each ES (CSC, WY, Ω), calculated using eq. 4, 5 or 6, we obtain a performance indicator *PI* for each erosion rate *e* at a site *s* in one of both scenarios by dividing the calculated *ES* by the maximum *ES* over the 5 erosion rates for this site:

$$PI_{ES,e,s}(-) = {ES_{e,s}} \Big/ {\max_{e=1..5} Es} \qquad [7]$$

2. A combined performance indicator *CPI* for each erosion rate, site and scenario is calculated by multiplication:

$$CPI_{e,s}(-) = PI_{(1-CSC),e,s} * PI_{wy,e,s} * PI_{\Omega,e,s} \qquad [8]$$

3. Results

3.1. Spatio-temporal trends in simulated climate and vegetation

Downscaled climate data (P and T) representative for the four sites are given in Fig. 2. In Fig. 2, year zero is the start of the precession cycle (SPC), the astronomical starting point of an interglacial, 22 ka indicates the end of the interglacial.

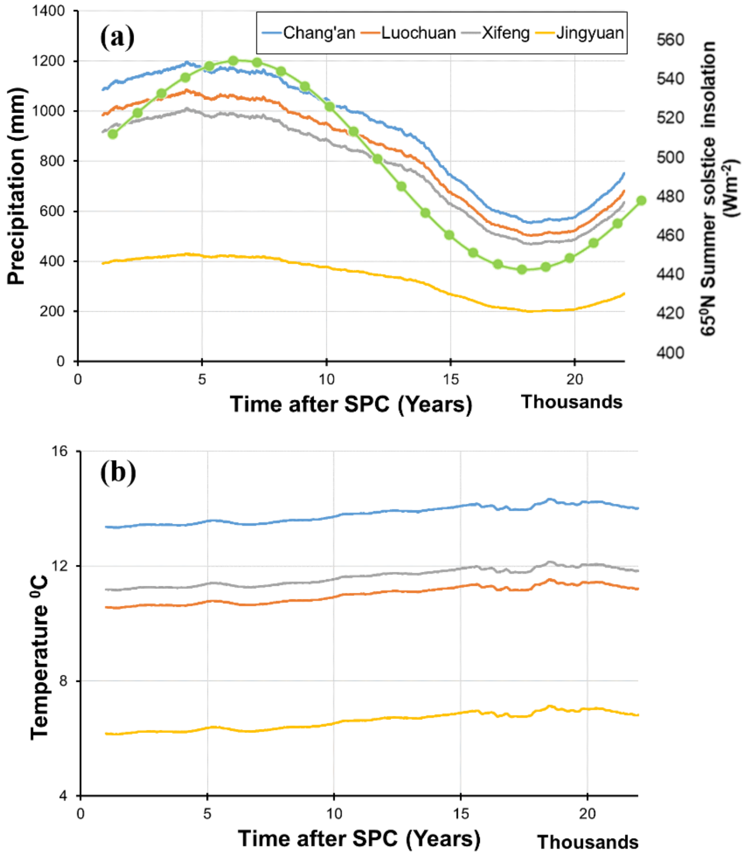

Figure. 2. Single column fitting image

Fig. 2. A 1000-year moving average applied to the simulated climatic data for the MIS 5e at the four locations: annual mean (a) precipitation (mm) and (b) temperature (˚C). Green dotted line indicates the summer insolation during MIS 5e.

The simulated climatic data capture the climatic gradient that prevails on the plateau during the entire Quaternary (Feng et al., 2004). Chang'an in the southeast receives the highest precipitation (on average 915 mm) whereas northwest located Jingyuan is characterized by the most strongly expressed semi-arid conditions, with the lowest precipitation (on average 330 mm) (Fig.2a). All four sites show a much wetter first half of the interglacial and a dryer second half. The variation of precipitation follows well the variation of the boreal summer insolation which depends strongly on the climatic precession and is the main controlling factor of the East Asian precipitation (Yin et al., 2009). The high precipitation in the first half of the simulation period corresponds to a time of high summer insolation, and the low precipitation in the second half of the simulation period corresponds to low summer insolation. The precipitation reaches a minimum about 18,000 years after SPC and increases again after. This is because summer insolation reaches a minimum about 18,000 years after SPC and increases after. This change in climate forcing has been well captured in the climate model. The annual mean temperature increases from Jingyuan to Chang'an, the 1000-year moving average ranging roughly from 6°C to 14°C (Fig. 2b). The highest mean temperatures occur during the second half of the interglacial at all sites.

Vegetation types (output at coarse scale of LOVECLIM) respond to the degree of aridity (Ep/P) at each particular site, and thus regional scale vegetation types differ along the climatic transect as well, both in space and time. During MIS 5e, deciduous forest is found in 96%, 85% and 61% of the years in Chang'an (wettest site), Luochuan, and Xifeng respectively. During the drier periods at each of these sites, grass/scrub vegetation is found. Jingyuan (driest site) by contrast predominantly has grass/scrub vegetation in 87% of the years, and deciduous forest in the less frequently occurring wetter periods.

3.2 Soil stocks evolution and SLT

3.2.1 Exchangeable Bases (EB)

Fig.3 presents the evolution of the absolute amounts of EB. For all the sites in both scenarios, the evolution of EB stock, for the duration of MIS 5e, can be explained by simulated soil profile distributions of calcite and total exchangeable bases, which are similar. As the CLP soils developed in calcite-rich loess parent material and calcite-rich added dust, the simulated EB were dominated by calcium ions in the soils. Also the initial exchangeable Ca^{+2} dominated the exchangeable bases (table S1). For all the sites in both scenarios, the calculated EB increases with erosion at the end of the interglacial (rightmost). The evolution of EB fluctuated depending on the total amount of base ions in the top soils, and a large decrease of bases can be related to loss of calcite. When soil erosion depletes calcite in the soils, the EB decreases (whiter areas), and if the top soil contains a calcite rich layer, the EB increases (darker areas).

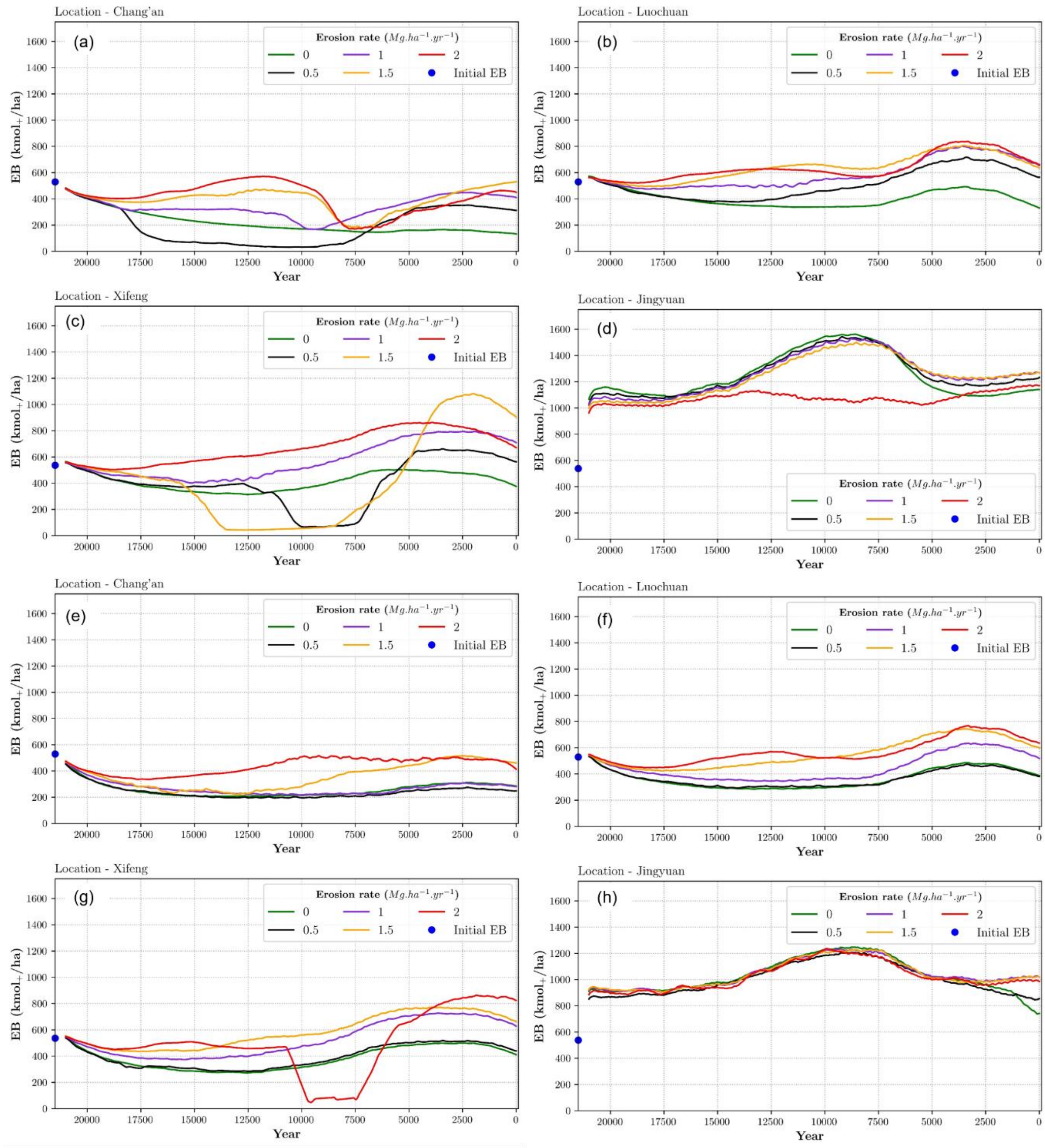

Figure. 3. Double (2) column fitting image

Fig. 3. Effect of natural erosion rates on EB evolution, in erosion-only (a, b, c, d) and dust addition plus erosion scenario (e, f, g, h). X-axis is simulation year and y-axis is scaled to 1600 kmol+/ha. A blue dot at the y-axis represents initial EB value determined by the parent material at the start of simulation. Colored lines denote different rates of erosion.

In erosion only scenario (location-Chang'an in Fig.3a), an erosion rate of 0.5 Mg ha^{-1} y^{-1} depletes the initial soils exchangeable bases because the litter layer is removed, which is a source of basic cations, and thus the base cation nutrient pump by the vegetation is weakened. The nutrient pump is not weakened at zero erosion. Simulated exchangeable bases (Fig.S2.a) and calcite profile distributions (see also Fig.S2.b) show very low bases in the top soils early in the time series (whiter areas in Figs.S2.a, b). At erosion rates above 0.5 Mg ha^{-1} y^{-1}, the calcite-rich layer is exposed by erosion in Chang'an (for example at 2.0 Mg ha^{-1} y^{-1} Figs.S2.c, d), and this leads to higher EB (Fig.3a).

In Xifeng (Fig.3c), EB during part of the interglacial is less than that at zero erosion for rates of 0.5 Mg ha^{-1} y^{-1} (Figs.S3.a, b), and 1.5 Mg ha^{-1} y^{-1} (Figs.S3.c, d). The weakened nutrient pump (removal of litter layer containing cations) and the depths of removal and accumulation of calcite are influencing the EB (Figs.S3), but not in a straightforward way because of interacting processes. However, at the end of the interglacial (rightmost), the net effect is that increasing erosion rates increase the EB, as in Chang'an, but values of EB at Xifeng are higher because the drier climate leads to shallower calcite accumulation and thus easier exposure by erosion (Figs.S3.e, f). In Jingyuan (Fig.3d), most of the EB are higher in the middle of the interglacial, while the EB lowers at 2.0 Mg ha^{-1} y^{-1} due to erosion in the top soils (Figs.S4.a, b).

Similarly, in the dust addition plus erosion scenario, the EB and calcite distribution together explain both the decrease and increase of EB in Xifeng at 2.0 Mg ha^{-1} y^{-1} (Fig.3g and Figs.S5. a, b, c, d). As mentioned before, in Jingyuan (Fig.3h), EB increases due to reaching calcite rich top soil layers at 1.5 and 2 Mg ha^{-1} y^{-1} erosion at the end of the interglacial (Figs.S6.a, b). At Jingyuan a little change of EB was observed over time and for different erosion rates in the first 20 ka (Fig.3h).

These findings suggest that depending on the initial amounts of bases, calcite contents in the parent material and in the added dust and the intensity of calcite leaching and clay migration processes in different locations together regulate exchangeable bases in the studied soils. The EB decreases from Jingyuan to Chang'an by following the climate gradient in the CLP. In general, the lowest EB was found at the moist Chang'an due to leaching of base cations from the surface soil and the highest EB is found at Jingyuan because of less leaching and intense loess accumulation.

Overall, our findings suggest that increasing erosion rates have a positive effect on exchangeable bases within the context of chosen natural erosion rates in the CLP soils. Table 1 represents rates of erosion with respect to EB, where major differences occur (increasing /decreasing) along the climatic gradient for each case (=SLT). In general, at the three sites with the most expressed summer monsoon (e.g. Chang'an, Luochuan and slightly in Xifeng), the SLT indicates the erosion rate above which EB increases due to reaching calcite-rich soil layers and at the most arid site (Jingyuan), the SLT indicates the erosion rate above which the EB decreases (or no effect of erosion).

Table 1. SLT values for EB for four locations.

EB	Chang'an	Luochuan	Xifeng	Jingyuan
	soil loss tolerance values (Mg $ha^{-1}y^{-1}$)			
Dust addition plus Erosion	Above 1.0	Above 0.5	Above 0.5	No effect
Erosion only	Above 0.5	Above 0	Above 1.0-1.5	Above 1.5

Table 1 and 2 data are based on cumulative stocks (see cumulative figures in supplementary materials) because absolute EB and SOC stocks show huge variations, making assessment of SLT difficult. As a conclusion, it can be stated that the temporal scale at which the SLT is assessed is influencing the uncertainty of the assessment.

3.2.2 Soil Organic Carbon (SOC)

Fig.4. presents the evolution of the absolute amounts of SOC. These SOC indicate a decrease of SOC at increasing erosion rate in the erosion-only (Fig.4.a, b, c and d) and in the dust addition plus erosion scenario (Fig.4.e, f, g and h), where the SOC-evolution pattern is ambiguous due to combined effects of both erosion and dust deposition, where dust deposition gradually buries the litter layer which then becomes incorporated in the soil.

The observed pulses in Fig.4 are due to both dust addition and soil erosion processes defined in the model. At an annual scale, dust addition first leads to a lower OC in the new top layer and buries the old top layer plus the litter layer below. Erosion removes the top layer and the litter layer and thus depletes SOC. Depicted as a moving average, these pulses are somewhat dampened. The simulated patterns of the effect of dust deposition and erosion on OC are presented in supplementary Fig.S7.

In addition, less SOC is a result of strong SOC decomposition at moist and warm locations such as Chang'an and Luochuan. Therefore, considering the location effect, the calculated SOC is minimal at Chang'an, due to high decomposition rates and the effect of the erosion rate is minimal (table 2). A high amount of SOC was modeled at Jingyuan, because of low decay rates in a cold and dry climate. However, on the other hand, precipitation is the variable that limits plant biomass production in the semi-arid northwestern CLP (Xu et al., 2007) such as Jingyuan in this study. Therefore, the simulated amounts of SOC in Jingyuan is probably high. Differences in plant biomass production varied, according to the downscaled LOVECLIM-simulations (see supplementary information), in Jingyuan (average 4.0 Mg ha^{-1} y^{-1}, grass/scrub vegetation) and Chang'an (average 7.0 Mg ha^{-1} y^{-1}, forest vegetation) and these influence the amount of SOC in the soil.

However, it is important to notice that the quantified Net Primary Production (NPP) varies with the different vegetation types and climate gradient in the studied sites as mentioned in section 3.1. In both scenarios, the increase of SOC between nearly 12500 and 5000 years (Jingyuan) and the last 7500 years of MIS 5e (Luochuan and Xifeng) is due to the dominance of grass/scrub vegetation in this period.

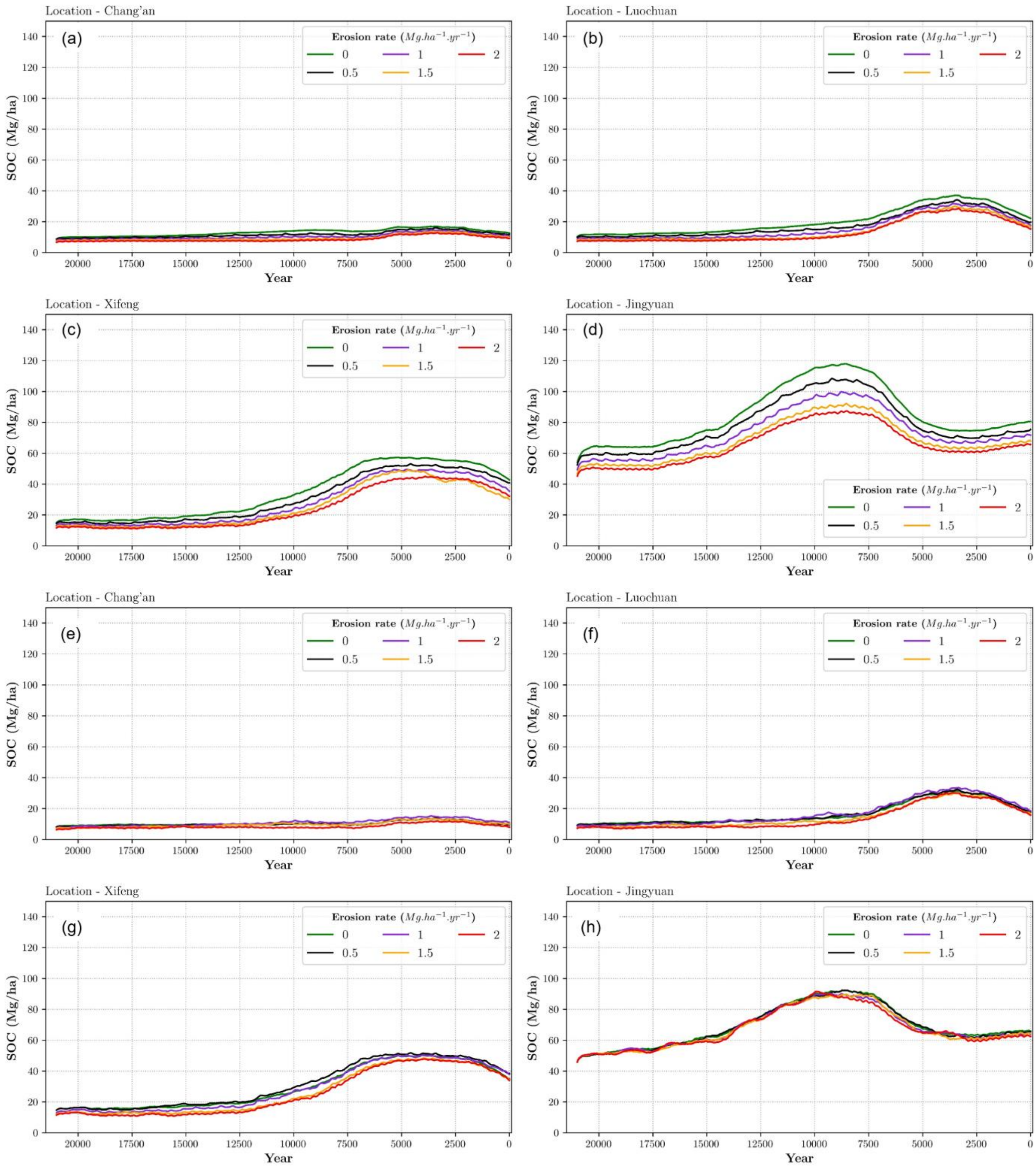

Figure. 4. Double (2) column fitting image

Fig. 4. Effect of natural erosion rates on SOC evolution, in erosion-only (a, b, c, d) and dust addition plus erosion scenario (e, f, g, h). X-axis is simulation year and y-axis is scaled to 140 Mg/ha. Colored lines denote different rates of erosion.

The SLT levels obtained for SOC along the climatic gradient are given in table 2 (based on cumulative SOC stocks). In the dust deposition plus erosion scenario erosion rates above 1.0

Mg ha^{-1} y^{-1} lead to reduced SOC. On the other hand, every rate of erosion above 0 Mg ha^{-1} y^{-1} in the erosion-only scenario has a negative effect on SOC as all the lines are clearly below the zero erosion rate (green line).

Table 2. SLT values for SOC for four locations.

SOC	Chang'an	Luochuan	Xifeng	Jingyuan
	soil loss tolerance values (Mg ha^{-1}y^{-1})			
	SOC decreases at			
Dust addition plus Erosion	Minimal effect	Above 1.0	Above 1.0	No effect
Erosion only	Above 0	Above 0	Above 0	Above 0

3.3 Soil ES evolution and SLT

3.3.1 Carbon Sequestration Capacity (CSC)

Fig.5. illustrates the evolution of the absolute amounts of CSC. In both scenarios, CSC increases at increasing rates of erosion. It is reasonable because soil erosion removes soil organic matter and provides the capacity to bind extra carbon in the remaining topsoil layers. The simulated SOC variations combined with the texture changes (Fig.S10) will determine the CSC fluctuations. Hence, the CSC graphs (Fig.5) resemble the SOC graphs (Fig.4).

The reason for higher CSC in Xifeng (Fig.5c) at 1.5 Mg ha^{-1} y^{-1} in the last 5000 years of MIS 5e is due to stronger decreasing SOC in the topsoils compared to 2.0 Mg ha^{-1} y^{-1} (see Fig.S8. a, b). This may perhaps be due to textural variations, which also affect CSC calculations (eq.3). In general, if the soil has high organic carbon content, CSC is low. Possibly, the dominance of grass/scrub vegetation and high OC in topsoils in Jingyuan shows zero CSC nearly between 12500 and 5000 years (Fig.5.d, h) and in Xifeng nearly in the last 7500 years of MIS 5e (Fig.5.c, g). It should be noted that our CSC only applies to the upper 30 cm and that the effect of off-site burial of SOC is not considered. In both scenarios (Fig.5), the CSC is decreasing from Chang'an, Luochuan, Xifeng to Jingyuan.

CSC differs between scenarios: lines in the erosion-only scenario (Fig.5.a, b, c and d) are further apart than in the dust addition+erosion scenario (Fig.5.e, f, g and h), indicating larger fluctuations of the quantity of CSC. The dust particles bind soil organic carbon due to (i) their fine texture (<20 µm; Hassink,1997) and (ii) binding on metal surfaces (e.g. Fe-oxides; Doetterl et al., 2018) in the added dust. In the present study, only the effect of the texture of the dust is included. Hence, in the dust+erosion scenario, the maximum carbon saturation value is changed according to soil texture changes, due to erosion of soil compartments, physical weathering and clay migration to deeper layers. Therefore, dust addition reduces the effect of erosion.

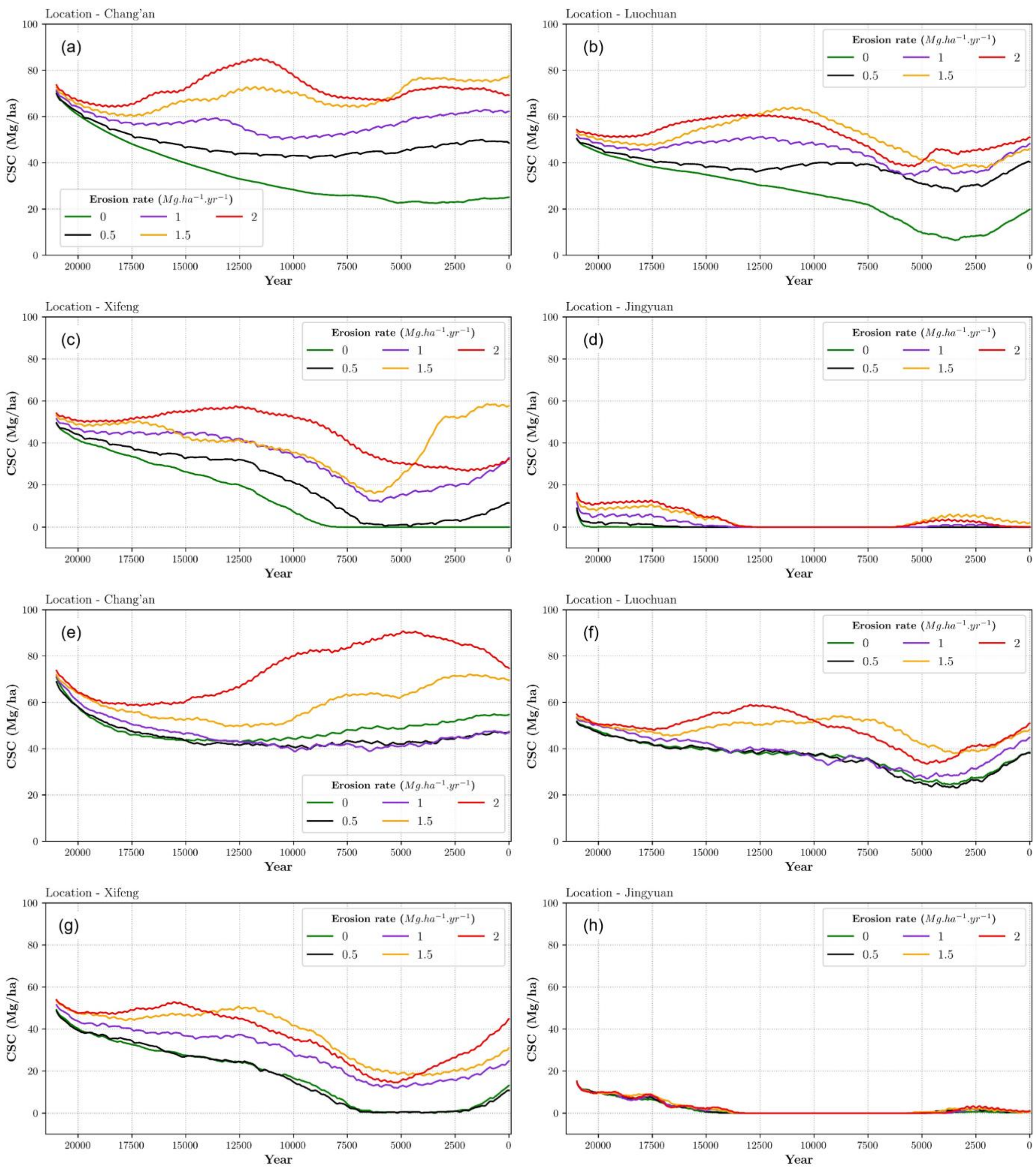

Figure. 5. Double (2) column fitting image

Fig. 5. Effect of natural erosion rates on CSC evolution, in erosion-only (a, b, c, d) and dust addition plus erosion scenario (e, f, g, h). X-axis is simulation year and y-axis is scaled to 100 Mg/ha. Colored lines denote different rates of erosion.

3.3.2 Water Yield (WY) and ratio actual/potential evapotranspiration (Ω)

The most important effect of erosion on WY (Fig.6) is that every rate of erosion above zero reduces the WY (=drainage) in both scenarios, and mostly relates to higher erosion rates: when the zone of export in soil is removed by erosion, a Bt horizon (clay-rich) exposes (Fig.S1). Therefore, we can assume that plant roots enter into the Bt horizon and enhance water uptake from the Bt, where more plant available water is present due to the higher clay content. As a result, there is less leaching of water and WY becomes low. In general, it should be noted that WY lowers towards the semi-arid sites because of low precipitation, and there is no important effect of different erosion rates on water yield at Jingyuan (Fig.6.d and h). Therefore, precipitation will restrict the WY in more arid (Jingyuan) relative to the moist locations (e.g. Chang'an) where soil properties (e.g. clay content) can play a role in determining the WY.

The impact of erosion rates on WY-evolution is less pronounced in the dust addition+erosion scenario (Fig.6.e, f, g and h) than in the erosion-only scenario (a strong reduction of water yield) (Fig.6.a, b, c and d). This may be due to the addition of dust containing fine materials which improves water retention, compensating topsoils removed by water erosion. Fig.6 shows overlapping lines near the end of the simulated interglacial (rightmost); this is due to the lower annual average precipitation simulated (Fig.2a). This suggests that the amount of precipitation largely determines the WY at the different erosion rates studied.

The ratio of actual over potential evapotranspiration, Ω, informs on how well water demand by vegetation is supplied by available soil water, and thus indicates if biomass production is stressed by soil water shortage. WY and Ω are not strictly inversely related, because not all soil water in the rooted zone is available for plants, and zero WY does not necessarily mean that plant water need is satisfied (see Fig.S9).

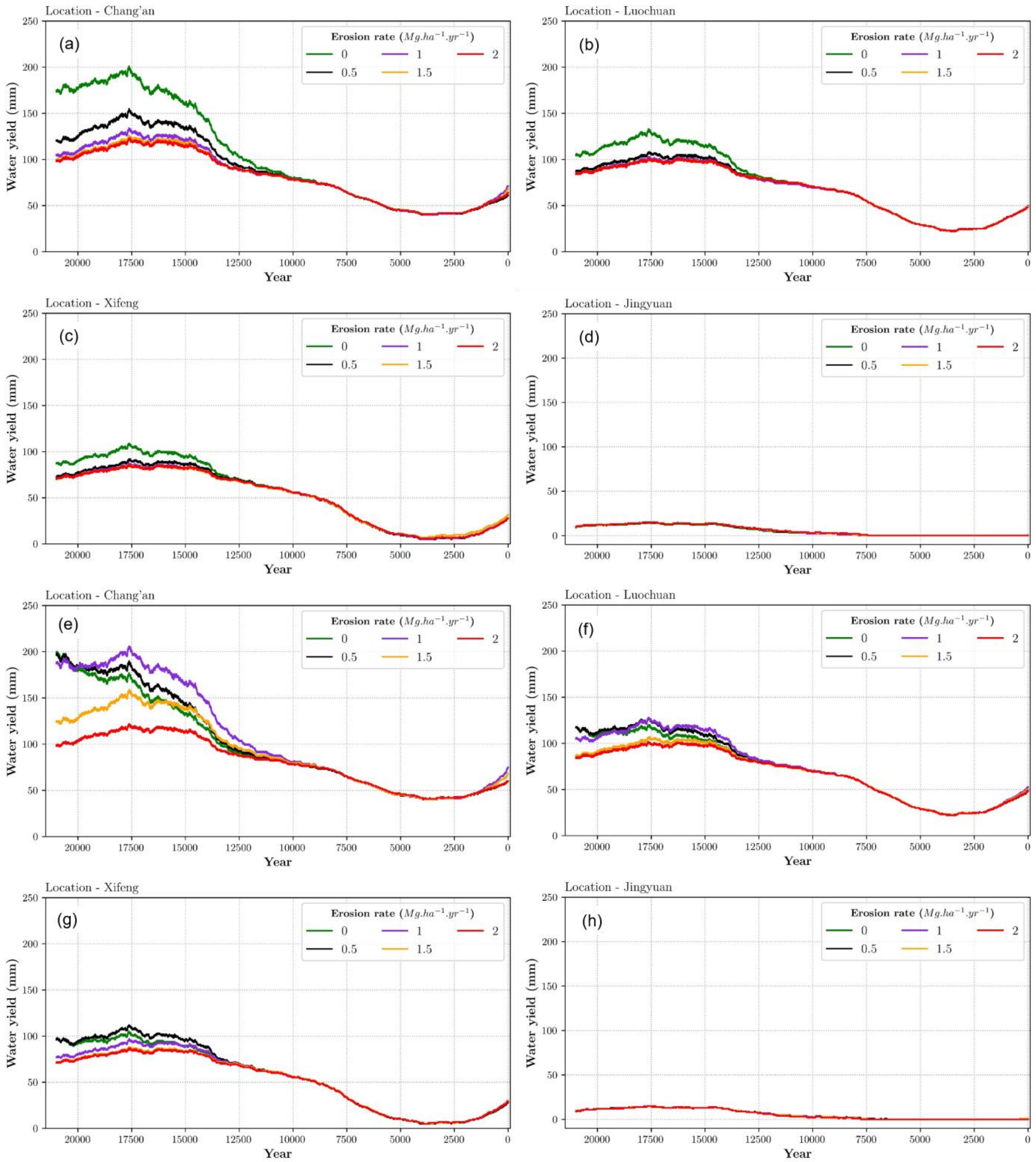

Figure. 6. Double (2) column fitting image

Fig. 6. Effect of natural erosion rates on WY evolution, in erosion-only (a, b, c, d) and dust addition plus erosion scenario (e, f, g, h). X-axis is simulation year and y-axis is scaled to 250 mm. Colored lines denote different rates of erosion.

3.3.3 Combining performance indices for ecosystem services

The combined performance indices for ES were calculated for the two scenarios at the five erosion rates by applying eq.7 for the ES: CSC, WY and Ω and then multiplying these indices using eq.8. The result in Fig.7 shows higher erosion rates (1.5 – 2.0 Mg ha^{-1} y^{-1}) influence the studied ecosystem services negatively, while lower erosion rates (0.5 – 1.0 Mg ha^{-1} y^{-1}) do not show a large negative impact. Like identified for the ES: CSC and WY in preceding sections, dust addition reduces the effect of erosion on ES at lower erosion rates. The ES performance is approximately constant in the dust addition plus erosion scenario (Fig.7a), whereas it is much more prominent in the erosion-only scenario (Fig.7b). For both scenarios, combined ES performance indicator showed a negative performance above 1.0 Mg ha^{-1} y^{-1}.

Fig.7b shows that the combined index is higher in erosion-only scenario than in the dust addition plus erosion scenario (Fig.7a) especially at lower erosion rates. The difference in the combined index is mainly due to the individual effect of the evolution of CSC, WY and Ω, which reflect the combined effect of soil forming factors, erosion and dust addition. For example, surprisingly, Jingyuan, shows a high index in erosion-only scenario (Fig.7b), due to its higher amount of SOC at lower erosion rates, compared to the other sites, while it is much lower in the dust addition plus erosion scenario (Fig.7a). These differences are attributed to simulated SOC and therefore CSC in soils. Erosion-only scenarios suggest a better soil ES performance at more arid sites at low erosion rates than at the two moist sites. However, focusing simply on erosion may overlook the relevance of knowing the correct plant biomass productivity and the relation between aridity and dust deposition.

Considering the simulated soil development and climate change under this study, we propose sites located near deserts would be considerably influenced by dust addition (e.g. Jingyuan) relative to the moister sites. Therefore, we stress that dust deposition and its composition are also important factors of SOC, CSC and SLT estimations.

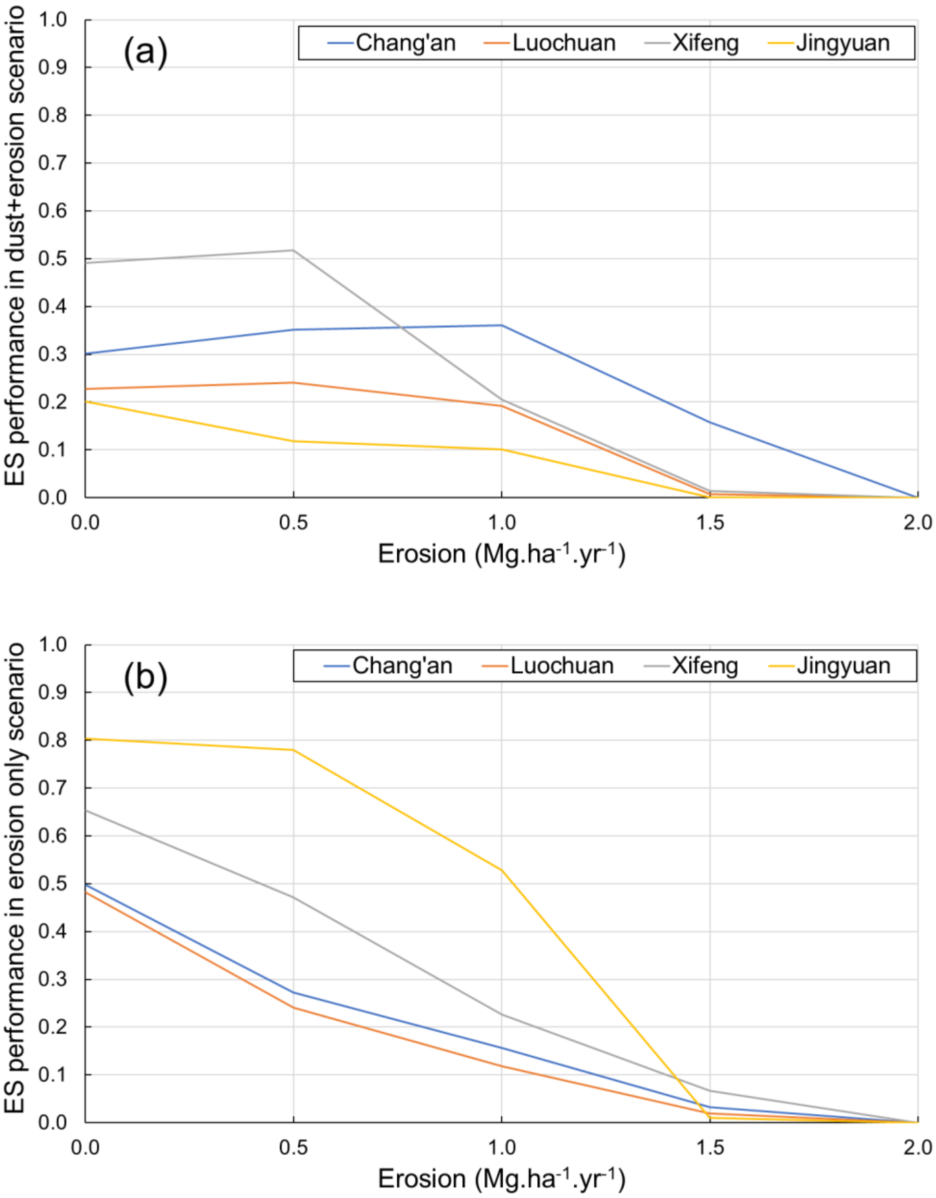

Figure. 7. Single column fitting image

Fig. 7. Combined performance indices for three simulated ecosystem services (1-CSC, WY and Ω per scenario) (a) dust+erosion and (b) erosion-only and per erosion rate for the simulation locations.

4. Discussion

(i) Concept of SLT under erosion/dust accumulation scenarios and semi-arid climate

Linking with the objectives, the variability in soil stocks and ES-performance was shown (Figs. 3, 4, 5, 6, 7) and causes were identified (Figs. S1, S2, S3, S4, S5, S6, S7, S8, S9, S10). Our simulation-based SLT and combined ES-performance indices confirm a difference between the two scenarios, where the erosion-only scenario shows wider differences in the combined index over lower erosion rates. In contrast, the differences are minor and approximately constant in the dust addition plus erosion scenario. Because of dust addition, for soil stocks, dust addition plus erosion scenario shows slightly higher SLT than erosion-only scenario. Our results show a clear sensitivity of the soil model outputs to different climate evolutions along the aridity transect, which allows for comparative scenario studies like we performed. Combined climate-soil evolution modeling is key to enabling such analyses. Based on the concept of SLT, at the low "natural" erosion rates under the semi-arid climate in this study, soil-based ES showed a negative performance above 1.0 Mg ha^{-1} y^{-1}, even though some stocks (SOC) respond negatively and (EB) respond positively above this rate.

Off-site effects of erosion may negatively affect water bodies and also change soil depth at accumulation locations. However, the studied erosion rates are low and would not produce a lot of colluvium, and the 1-D soil model does not allow to calculate mass redistribution over a landscape. For these reasons, we did not include erosion modeling nor discussed off-site problems. The only way that we see to include off-site effects, is to add a separate series of scenarios of colluviation, which would probably be an enrichment to the study but is also not easily done. We did not include this, also because off-site effects are of impact under agricultural land use but much less under natural vegetation as in MIS 5e.

(ii) Potential applications of the modeling approach for SLT

Understanding SLT in a managed land-use context is another important aspect. SLT would be calculated for higher, man-induced erosion rates. An extension of this study towards higher erosion rates might be useful to identify tipping points, erosion rates that will result in loss of performance when exceeded. For future application of the present study in an Anthropocene perspective, appropriate (shorter) time-scales need to be chosen, especially when simulations are linked to field studies. The natural (e.g. climate, erosion, and deposition) and human intervention (e.g. land-use types, agricultural practices: slash burn cultivation, tillage, irrigation, fertilization) factors must be assessed in the modeling. Therefore, a future study should satisfy time series data needs in a managed land-use context. Besides that, model calibration is also an important step.

(iii) Soil-climate modeling and SLT

Our results showed climate is an important driver in SLT quantifications. Therefore, time series of climate data are required to understand the “soil change” for a given location. Understanding “soil change” is vital in determining the soil status for supplying soil stocks and ES, which change under different climatic conditions (precipitation, temperature). Therefore, it is increasingly necessary to integrate soil changes with other components (hydrosphere, lithosphere, atmosphere, and biosphere) of the earth system to obtain a better understanding of soil processes, ES, and globally concerning matters such as SLT. Therefore, we propose that soil-climate modeling approaches provide a better framework that can fully capture the role of soils in a coupled system.

(iv) Limitations of this study

Some methodological flaws appear in the studied soil model-based ecosystem services assessment. In this study, the CSC estimation is influenced by the SOC level in the simulated soil. SOC and CSC are interlinked. In this study, the annual addition of organic carbon by plants (site- and climate-specific) is an input parameter and estimated by mean annual temperature and precipitation over four sites in the CLP. Even though a variety of factors naturally influences root depths (e.g. soil, climate, vegetation), the current model simulates plant water uptake and the fraction of roots (and root input organic matter) over the soil compartments per year by employing a root density function (roots exponentially decrease with depths). We use a maximum (100 cm) root depth for forests, which is the depth of the initial profile and hence is the maximum value that can be given, and reasonably its half value of 50 cm is allocated for grass/scrubs vegetation. When true maximum rooting depths would exceed 1 meter, the vast majority of roots and associated water uptake would still be in the upper meter, so we expect little impact on our results. Despite unavoidable uncertainties in data from paleoclimate simulations, it is worth noting here we corrected for systematic biases (see supplementary information). Reconstructing the climate using proxies would suffer from similar larger uncertainties. Moreover, as we applied the 1-D model, erosion is considered a completely independent external-input with no connection to the rainfall intensity in the area. The majority of ES studies (e.g. Di et al., 2017; Su et al., 2018; Wang et al., 2011) in the loess plateau focus on agricultural production purposes, considering climate change/gradients, land cover, land-use change and revegetation. However, we studied all the soil stocks and ES solely to evaluate how those evolve under natural vegetations. Thus, evaluating soil quality based on these indices from an agricultural productivity perspective is beyond the scope of this study, and it must be noted as well that the study concerns MIS 5e. Finally, the SLT at various erosion rates are estimated for a semi-arid, monsoon-type climate evolution. The found SLT are therefore bound to these climates.

5. Conclusions

In this paper, we test a new modeling approach for estimating selected soil stocks and ES and assessing possible SLT in four locations on the CLP over 22 ka. We show the importance of mechanistic soil modeling for quantifying ES as the initial step for assessing ES. We stress that mathematical modeling is a better option for assessment of soil stocks (natural capital) and ES than common inventory-based studies, for a number of reasons: (i) stocks and ES can be quantified; (ii) past, present and future situations can be quantified; (iii) effects of scenarios of the forcing factors (e.g. climate, erosion) can be studied; (iv) while extrapolation of data inventory based assessments is risky, extrapolations using mechanistic instruments are less risky. Because physical laws like the conservation of mass, potential-driven water and solute flow constrain the results even when boundary conditions become extreme (e.g. high rainfall), while empirical relations are risky to be applied outside their domain.

The main findings are:

(i) Two soil stocks, EB and SOC, respond differently to increased erosion. Whereas SOC decreases when erosion occurs, usually EB increases with erosion in both scenarios, in response to huge variations in calcium-rich horizons that become part of the topsoil over the modeling period.

(ii) Three ecosystem services, CSC, WY and Ω respond differently to increased erosion. SLT, as assessed by the combined ES performance indicator, showed a negative performance above 1.0 Mg ha^{-1} y^{-1}. This SLT-threshold is bound to the studied (semi-arid, monsoon) climate evolution.

(iii) SLT benchmark levels should be chosen carefully based on analysis of the effect of natural erosion rates.

(iv) Dust deposition may obscure the effect of erosion in ES performance, however, it must be studied further.

Acknowledgement

This work is supported by the Fonds de la Recherche Scientifique-FNRS (F.R.S.-FNRS) under grant MIS F.4529.18. Q.Z. Yin is Research Associate of F.R.S.-FNRS. We are grateful to Dr. Hao Lu for his assistance in modifying the map of the CLP of this manuscript.

Declaration of Competing Interest

The authors declare that they have no known competing financial interests or personal relationships that could have appeared to influence the work reported in this paper.

Appendix A. Supplementary data

Supplementary data to this article can be found online at https:// doi.org/10.1016/j.gloplacha.2021.103548.

References

Adhikari, K., Hartemink, A.E., 2016. Linking soils to ecosystem services - A global review. Geoderma 262, 101–111. https://doi.org/10.1016/j.geoderma.2015.08.009

Alewell, C., Egli, M., Meusburger, K., 2015. An attempt to estimate tolerable soil erosion rates by matching soil formation with denudation in Alpine grasslands. J. Soils Sediments 15, 1383–1399. https://doi.org/10.1007/s11368-014-0920-6

An, Z., Kukla, G.J., Porter, S.C., Xiao, J., 1991. Magnetic susceptibility evidence of monsoon variation on the Loess Plateau of central China during the last 130,000 years. Quat. Res. 36, 29–36. https://doi.org/10.1016/0033-5894(91)90015-W

An, Z., Tunghseng, L., Yanchou, L., Porter, S.C., Kukla, G., Xihaoll, W., Yingming, H., 1990. The long-term paleomonsoon variation recorded by the loess-paleosol sequence in Central China. Quat. Int. 7–8, 91–95. https://doi.org/10.1016/1040-6182(90)90042-3

Angers, D.A., Arrouays, D., Saby, N.P.A., Walter, C., 2011. Estimating and mapping the carbon saturation deficit of French agricultural topsoils. Soil Use Manag. 27, 448–452. https://doi.org/https://doi.org/10.1111/j.1475-2743.2011.00366.x

Bazzoffi, P., 2009. Soil erosion tolerance and water runoff control: Minimum environmental standards. Reg. Environ. Chang. 9, 169–179. https://doi.org/10.1007/s10113-008-0046-8

Boardman, J., Poesen, J., 2006. Soil Erosion in Europe: Major Processes, Causes and Consequences, in: Boardman, J., Poesen, J. (Eds.), Soil Erosion in Europe. John Wiley & Sons, Ltd, Chichester, UK, pp. 477–487. https://doi.org/10.1002/0470859202

Bouma, J., 2014. Soil science contributions towards Sustainable Development Goals and their implementation: Linking soil functions with ecosystem services. J. Plant Nutr. Soil Sci. 177, 111–120. https://doi.org/10.1002/jpln.201300646

Cai, Q., 2001. Soil erosion and management on the Loess Plateau. J. Geogr. Sci. 11, 53–70. https://doi.org/10.1007/BF02837376

Calzolari, C., Ungaro, F., Filippi, N., Guermandi, M., Malucelli, F., Marchi, N., Staffilani, F., Tarocco, P., 2016. A methodological framework to assess the multiple contributions of soils to ecosystem services delivery at regional scale. Geoderma 261, 190–203. https://doi.org/10.1016/j.geoderma.2015.07.013

Costanza, R., D'Arge, R., De Groot, R., Farber, S., Grasso, M., Hannon, B., Limburg, K., Naeem, S., O'Neill, R. V., Paruelo, J., Raskin, R.G., Sutton, P., Van Den Belt, M., 1997. The value of the world's ecosystem services and natural capital. Nature 387, 253–260. https://doi.org/10.1038/387253a0

Daily, G.C., Matson, P.A., Vitousek, P.M., 1997. Ecosystem services supplied by soil, in: Daily, G. (Ed.), Nature's Services: Societal Dependence on Natural Ecosystems. Island press, Washington, DC, pp. 113–132.

DeGroot, R.S., Wilson, M.A., Boumans, R.M.J., 2002. A typology for the classification, description and valuation of ecosystem functions, goods and services. Ecol. Econ. 41, 393–408. https://doi.org/10.1016/S0921-8009(02)00089-7

Di, J., Feng, W., Zhang, W., Cai, A., Xu, M., 2017. Soil organic carbon saturation deficit under primary agricultural managements across major croplands in China. Ecosyst. Heal. Sustain. 3. https://doi.org/10.1080/20964129.2017.1364047

Ding, Z.L., Derbyshire, E., Yang, S.L., Yu, Z.W., Xiong, S.F., Liu, T.S., 2002. Stacked 2.6-Ma grain size record from the Chinese loess based on five sections and correlation with the deep-sea δ 18 O record . Paleoceanography 17, 5-1-5–21. https://doi.org/10.1029/2001pa000725

DiStefano, C., Ferro, V., 2016. Establishing soil loss tolerance: An overview. J. Agric. Eng. 47, 127–133. https://doi.org/10.4081/jae.2016.560

Doetterl, S., Berhe, A.A., Arnold, C., Bodé, S., Fiener, P., Finke, P., Fuchslueger, L., Griepentrog, M., Harden, J.W., Nadeu, E., Schnecker, J., Six, J., Trumbore, S., Van Oost, K., Vogel, C., Boeckx, P., 2018. Links among warming, carbon and microbial dynamics mediated by soil mineral weathering. Nat. Geosci. 11, 589–593. https://doi.org/10.1038/s41561-018-0168-7

Dominati, E., Mackay, A., Green, S., Patterson, M., 2014. A soil change-based methodology for the quantification and valuation of ecosystem services from agro-ecosystems: A case study of pastoral agriculture in New Zealand. Ecol. Econ. 100, 119–129. https://doi.org/10.1016/j.ecolecon.2014.02.008

Dominati, E., Patterson, M., Mackay, A., 2010. A framework for classifying and quantifying the natural capital and ecosystem services of soils. Ecol. Econ. 69, 1858–1868. https://doi.org/10.1016/j.ecolecon.2010.05.002

Duan, X., Shi, X., Li, Y., Rong, L., Fen, D., 2017. A new method to calculate soil loss tolerance for sustainable soil productivity in farmland. Agron. Sustain. Dev. 37. https://doi.org/10.1007/s13593-016-0409-3

Feng, Q., Zhao, W., Hu, X., Liu, Y., Daryanto, S., Cherubini, F., 2020. Trading-off ecosystem services for better ecological restoration: A case study in the Loess Plateau of China. J. Clean. Prod. 257, 120469. https://doi.org/10.1016/j.jclepro.2020.120469

Feng, Q., Zhao, W., Wang, J., Zhang, X., Zhao, M., Zhong, L., Liu, Y., Fang, X., 2016. Effects of Different Land-Use Types on Soil Erosion Under Natural Rainfall in the Loess Plateau, China. Pedosphere 26, 243–256. https://doi.org/10.1016/S1002-0160(15)60039-X

Feng, W., Plante, A.F., Six, J., 2013. Improving estimates of maximal organic carbon stabilization by fine soil particles. Biogeochemistry 112, 81–93. https://doi.org/10.1007/s10533-011-9679-7

Feng, Z.D., Wang, H.B., Olson, C., Pope, G.A., Chen, F.H., Zhang, J.W., An, C.B., 2004. Chronological discord between the last interglacial paleosol (S1) and its parent material in the Chinese Loess Plateau. Quat. Int. 117, 17–26. https://doi.org/10.1016/S1040-6182(03)00112-5

Finke, P.A., 2020. SOILGEN: A simulation model for soil development in various parent materials. Dept. Environment, Ghent, Belgium.

Finke, P.A., 2012. Modeling the genesis of luvisols as a function of topographic position in loess parent material. Quat. Int. 265, 3–17. https://doi.org/10.1016/j.quaint.2011.10.016

Finke, P.A., Hutson, J.L., 2008. Modelling soil genesis in calcareous loess. Geoderma 145, 462–479. https://doi.org/10.1016/j.geoderma.2008.01.017

Finke, P.A., Jafari, A., Zwertvaegher, A., Thas, O., 2018. Quantifying the uncertainty of a model-reconstructed soilscape for archaeological land evaluation. Geoderma 320, 74–81. https://doi.org/10.1016/j.geoderma.2018.01.032

Finke, P.A., Ranathunga Arachchige, K.N., Verdoodt, A., Yu, Y.Y., Yin, Q.Z., 2021. Unraveling loess records of climate change from the Chinese loess plateau using process-based models, in: Hunt, A., Egli, M., Faybishenko, B. (Eds.), Hydrogeology, Chemical Weathering and Soil Formation. AGU Geophysical Monograph Series, pp.

163–175. https://doi.org/10.1002/9781119563952.ch8

Finke, P.A., Samouëlian, A., Suarez-Bonnet, M., Laroche, B., Cornu, S.S., 2015. Assessing the usage potential of SoilGen2 to predict clay translocation under forest and agricultural land uses. Eur. J. Soil Sci. 66, 194–205. https://doi.org/10.1111/ejss.12190

Finke, P.A., Yin, Q.Z., Bernardini, N.J., Yu, Y., 2017. Climate-soil model reveals causes of differences between Marine Isotope Stage 5e and 13 paleosols. Geology 46, 99–102. https://doi.org/10.1130/G39301.1

Fossey, M., Angers, D., Bustany, C., Cudennec, C., Durand, P., Gascuel-Odoux, C., Jaffrezic, A., Pérès, G., Besse, C., Walter, C., 2020. A Framework to Consider Soil Ecosystem Services in Territorial Planning. Front. Environ. Sci. 8, 1–13. https://doi.org/10.3389/fenvs.2020.00028

Goosse, H., Brovkin, V., Fichefet, T., Haarsma, R., Huybrechts, P., Jongma, J., Mouchet, A., Selten, F., Barriat, P.Y., Campin, J.M., Deleersnijder, E., Driesschaert, E., Goelzer, H., Janssens, I., Loutre, M.F., Morales Maqueda, M.A., Opsteegh, T., Mathieu, P.P., Munhoven, G., Pettersson, E.J., Renssen, H., Roche, D.M., Schaeffer, M., Tartinville, B., Timmermann, A., Weber, S.L., 2010. Description of the Earth system model of intermediate complexity LOVECLIM version 1.2. Geosci. Model Dev. 3, 603–633. https://doi.org/10.5194/gmd-3-603-2010

Granger, D.E., Kirchner, J.W., Finkel, R., 1996. Spatially Averaged Long-Term Erosion Rates Measured from in Situ-Produced Cosmogenic Nuclides in Alluvial Sediment. J. Geol. 104, 249–257.

Greiner, L., Keller, A., Grêt-Regamey, A., Papritz, A., 2017. Soil function assessment: review of methods for quantifying the contributions of soils to ecosystem services. Land use policy 69, 224–237. https://doi.org/10.1016/j.landusepol.2017.06.025

Guo, Z.T., Biscaye, P., Wei, L., Chen, X., Peng, S., Liu, T., 2000. Summer monsoon variations over the last 1.2 Ma from the weathering of loess-soil sequences in China. Geophys. Res. Lett. 27, 1751–1754. https://doi.org/10.1029/1999GL008419

Guo, Z.T., Ruddiman, W.F., Hao, Q.Z., Wu, H.B., Qiao, Y.S., Zhu, R.X., Peng, S.Z., Wel, J.J., Yuan, B.Y., Llu, T.S., Wei, J.J., Yuan, B.Y., Liu, T.S., 2002. Onset of Asian desertification by 22 Myr ago inferred from loess deposits in China. Nature 416, 159–163. https://doi.org/10.1038/416159a

Han, J., Fyfe, W.S., Longstaffe, F.J., 1998. Climatic implications of the S5 Paleosol Complex on the southernmost Chinese Loess Plateau. Quat. Res. 50, 21–33. https://doi.org/10.1006/qres.1998.1976

Hao, Q., Guo, Z., 2005. Spatial variations of magnetic susceptibility of Chinese loess for the last 600 kyr: Implications for monsoon evolution. J. Geophys. Res. Solid Earth 110, 1–10. https://doi.org/10.1029/2005JB003765

Hassink, J., 1997. The capacity of soils to preserve organic C and N by their association with clay and silt particles. Plant Soil 191, 77–87. https://doi.org/10.1023/A:1004213929699

Hewitt, A., Dominati, E., Webb, T., Cuthill, T., 2015. Soil natural capital quantification by the stock adequacy method. Geoderma 241–242, 107–114. https://doi.org/10.1016/j.geoderma.2014.11.014

Jenny, H., 1941. Factors of Soil Formation. A System of Quantitative Pedology. McGraw-Hill Book Company, New York, London.

Jeong, G.Y., Hillier, S., Kemp, R.A., 2011. Changes in mineralogy of loess–paleosol sections across the Chinese Loess Plateau. Quat. Res. 75, 245–255. https://doi.org/10.1016/j.yqres.2010.09.001

Jiang, W., Yang, X., Cheng, Y., 2014. Spatial patterns of vegetation and climate on the Chinese Loess Plateau since the Last Glacial Maximum. Quat. Int. 334–335, 52–60. https://doi.org/10.1016/j.quaint.2013.10.039

Jun, C., Junfeng, J., Gang, Q., 1998. Geochemical studies on the intensity of chemical weathering in Luochuan loess-paleosol sequence, China. Sci. China Ser. D-Earth Sci. 41(3), 235–241. https://doi.org/10.1007/BF02973110

Kemp, R.A., 2001. Pedogenic modification of loess: Significance for palaeoclimatic reconstructions. Earth-Science Rev. 54, 145–156. https://doi.org/10.1016/S0012-8252(01)00045-9

Keyvanshokouhi, S., Cornu, S., Samouëlian, A., Finke, P., 2016. Evaluating SoilGen2 as a tool for projecting soil evolution induced by global change. Sci. Total Environ. 571, 110–123. https://doi.org/10.1016/j.scitotenv.2016.07.119

Kukla, G., 1987. Loess stratigraphy in central China. Quat. Sci. Rev. 6, 191–207, 209–219. https://doi.org/10.1016/0277-3791(87)90004-7

Lang, Y., Song, W., Zhang, Y., 2017. Responses of the water-yield ecosystem service to climate and land use change in Sancha River Basin, China. Phys. Chem. Earth 101, 102–111. https://doi.org/10.1016/j.pce.2017.06.003

Li, L., Du, S., Wu, L., Liu, G., 2009. An overview of soil loss tolerance. Catena 78, 93–99. https://doi.org/10.1016/j.catena.2009.03.007

Li, Z., Nie, X., Chang, X., Liu, L., Sun, L., 2016. Characteristics of soil and organic carbon loss induced by water erosion on the loess plateau in China. PLoS One 11, 1–13. https://doi.org/10.1371/journal.pone.0154591

Liu, T.., 1985. Loess and the Environment. China Ocean Press, Beijing.

Liu, Z., Shao, M., Wang, Y., 2011. Effect of environmental factors on regional soil organic carbon stocks across the Loess Plateau region, China. Agric. Ecosyst. Environ. 142, 184–194. https://doi.org/10.1016/j.agee.2011.05.002

Lu, H., Sun, D., 2000. Pathways of dust input to the Chinese Loess Plateau during the last glacial and interglacial periods. Catena 40, 251–261. https://doi.org/10.1016/S0341-8162(00)00090-4

Lu, N., Akujärvi, A., Wu, X., Liski, J., Wen, Z., Holmberg, M., Feng, X., Zeng, Y., Fu, B., 2015. Changes in soil carbon stock predicted by a process-based soil carbon model (Yasso07) in the Yanhe watershed of the Loess Plateau. Landsc. Ecol. 30, 399–413. https://doi.org/10.1007/s10980-014-0132-x

Maher, B.A., Thompson, R., 1991. Mineral magnetic record of the Chinese loess and paleosols. Geology 19, 3–6. https://doi.org/10.1130/0091-7613(1991)019<0003:MMROTC>2.3.CO;2

MEA, 2005. Ecosystems and human well-being: Synthesis. Island press, Washington, DC.

Muri, H., Berger, A., Yin, Q.Z., Karami, M.P., Barriat, P.Y., 2013. The climate of the MIS-13 interglacial according to HadCM3. J. Clim. 26, 9696–9712. https://doi.org/10.1175/JCLI-D-12-00520.1

Nearing, M.A., Xie, Y., Liu, B., Ye, Y., 2017. Natural and anthropogenic rates of soil erosion. Int. Soil Water Conserv. Res. 5, 77–84. https://doi.org/10.1016/j.iswcr.2017.04.001

Rutgers, M., van Wijnen, H.J., Schouten, A.J., Mulder, C., Kuiten, A.M.P., Brussaard, L., Breure, A.M., 2012. A method to assess ecosystem services developed from soil attributes with stakeholders and data of four arable farms. Sci. Total Environ. 415, 39–48. https://doi.org/10.1016/j.scitotenv.2011.04.041

Sauer, D., Finke, P., Sørensen, R., Sperstad, R., Schülli-Maurer, I., Høeg, H., Stahr, K., 2012. Testing a soil development model against southern Norway soil chronosequences. Quat. Int. 265, 18–31. https://doi.org/10.1016/j.quaint.2011.12.018

Shi, H., Shao, M., 2000. Soil and water loss from the Loess Plateau in China. J. Arid Environ. 45, 9–20. https://doi.org/10.1006/jare.1999.0618

Six, J., Conant, R.T., Paul, E.A., Paustian, K., 2002. Stabilization mechanisms of soil organic matter: Implications for C-saturation of soils. Plant Soil 241, 155–176. https://doi.org/10.1023/A:1016125726789

Sparovek, G., De Maria, I.C., 2003. Multiperspective analysis of erosion tolerance. Sci. Agric. 60, 409–416. https://doi.org/10.1590/S0103-90162003000200029

Stewart, C.E., Paustian, K., Conant, R.T., Plante, A.F., Six, J., 2007. Soil carbon saturation: Concept, evidence and evaluation. Biogeochemistry 86, 19–31. https://doi.org/10.1007/s10533-007-9140-0

Su, C., Fu, B.J., He, C.S., Lü, Y.H., 2012. Variation of ecosystem services and human activities: A case study in the Yanhe Watershed of China. Acta Oecologica 44, 46–57. https://doi.org/10.1016/j.actao.2011.11.006

Su, C., Liu, H., Wang, S., 2018. A process-based framework for soil ecosystem services study and management. Sci. Total Environ. 627, 282–289. https://doi.org/10.1016/j.scitotenv.2018.01.244

Vereecken, H., Schnepf, A., Hopmans, J.W., Javaux, M., Or, D., Roose, T., Vanderborght, J., Young, M.H., Amelung, W., Aitkenhead, M., Allison, S.D., Assouline, S., Baveye, P., Berli, M., Brüggemann, N., Finke, P., Flury, M., Gaiser, T., Govers, G., Ghezzehei, T., Hallett, P., Hendricks Franssen, H.J., Heppell, J., Horn, R., Huisman, J.A., Jacques, D., Jonard, F., Kollet, S., Lafolie, F., Lamorski, K., Leitner, D., McBratney, A., Minasny, B., Montzka, C., Nowak, W., Pachepsky, Y., Padarian, J., Romano, N., Roth, K., Rothfuss, Y., Rowe, E.C., Schwen, A., Šimůnek, J., Tiktak, A., Van Dam, J., van der Zee, S.E.A.T.M., Vogel, H.J., Vrugt, J.A., Wöhling, T., Young, I.M., 2016. Modeling Soil Processes: Review, Key Challenges, and New Perspectives. Vadose Zo. J. 15, vzj2015.09.0131. https://doi.org/10.2136/vzj2015.09.0131

Verheijen, F.G.A., Jones, R.J.A., Rickson, R.J., Smith, C.J., 2009. Tolerable versus actual soil erosion rates in Europe. Earth-Science Rev. 94, 23–38. https://doi.org/10.1016/j.earscirev.2009.02.003

Wang, Y., Fu, B., Lü, Y., Chen, L., 2011. Effects of vegetation restoration on soil organic carbon sequestration at multiple scales in semi-arid Loess Plateau, China. Catena 85, 58–66. https://doi.org/10.1016/j.catena.2010.12.003

Wilkinson, B.H., McElroy, B.J., 2007. The impact of humans on continental erosion and sedimentation. Bull. Geol. Soc. Am. 119, 140–156. https://doi.org/10.1130/B25899.1

Wischmeier, W.H., Smith, D.D., 1979. Predicting rainfall-erosion losses from cropland east of the Rocky mountains-Guide for Selection of Practices for Soil and Water Conservation, in: Agricultural Handbook 282. U.S Department of Agriculture, Washington.

Xiong, S., Ding, Z., Zhu, Y., Zhou, R., Lu, H., 2010. A ~6Ma chemical weathering history, the grain size dependence of chemical weathering intensity, and its implications for provenance change of the Chinese loess-red clay deposit. Quat. Sci. Rev. 29, 1911–1922. https://doi.org/10.1016/j.quascirev.2010.04.009

Xu, B., Shan, L., Li, F., Jiang, J., 2007. Seasonal and spatial root biomass and water use efficiency of four forage legumes in semiarid northwest China. African J. Biotechnol. 6, 2708–2714. https://doi.org/10.5897/AJB2007.000-2433

Yamanaka, N., Hou, Q.-C., Sheng, D., Du, S., 2014. Vegetation of the Loess Plateau, in: Tsunekawa, A., Liu, G., Yamanaka, N., Du, S. (Eds.), Restoration and Development of the Degraded Loess Plateau,China. Springer Japan, pp. 49–60. https://doi.org/10.1007/978-4-431-54481-4_4

Yang, S., Ding, Z., 2008. Advance-retreat history of the East-Asian summer monsoon rainfall belt over northern China during the last two glacial-interglacial cycles. Earth Planet. Sci. Lett. 274, 499–510. https://doi.org/10.1016/j.epsl.2008.08.001

Yang, S., Ding, Z., Wang, X., Tang, Z., Gu, Z., 2012. Negative δ 18O-δ 13C relationship of pedogenic carbonate from northern China indicates a strong response of C 3/C 4 biomass to the seasonality of Asian monsoon precipitation. Palaeogeogr. Palaeoclimatol.

Palaeoecol. 317–318, 32–40. https://doi.org/10.1016/j.palaeo.2011.12.007

Yin, G., Wang, X., Zhang, X., Fu, Y., Hao, F., Hu, Q., 2020. InVEST model-based estimation of water yield in North China and its sensitivities to climate variables. Water (Switzerland) 12. https://doi.org/10.3390/W12061692

Yin, Q.Z., Berger, A., 2015. Interglacial analogues of the Holocene and its natural near future. Quat. Sci. Rev. 120, 28–46. https://doi.org/10.1016/j.quascirev.2015.04.008

Yin, Q.Z., Berger, A., 2012. Individual contribution of insolation and CO2 to the interglacial climates of the past 800,000 years. Clim. Dyn. 38, 709–724. https://doi.org/10.1007/s00382-011-1013-5

Yin, Q.Z., Berger, A., Crucifix, M., 2009. Individual and combined effects of ice sheets and precession on MIS-13 climate. Clim. Past 5, 229–243. https://doi.org/10.5194/cp-5-229-2009

Yu, Y.Y., Finke, P.A., Wu, H.B., Guo, Z.T., 2013. Sensitivity analysis and calibration of a soil carbon model (SoilGen2) in two contrasting loess forest soils. Geosci. Model Dev. 6, 29–44. https://doi.org/10.5194/gmd-6-29-2013

Zwertvaegher, A., Finke, P., De Smedt, P., Gelorini, V., Van Meirvenne, M., Bats, M., De Reu, J., Antrop, M., Bourgeois, J., De Maeyer, P., Verniers, J., Crombé, P., 2013. Spatio-temporal modeling of soil characteristics for soilscape reconstruction. Geoderma 207–208, 166–179. https://doi.org/10.1016/j.geoderma.2013.05.013